Power Electronics and Drives
Volume 7(42), 2022 DOI: 10.2478/pead-2022-0020

Power Electronics and Drives

Universal System for Detection and Compensation of Current Sensor Faults in Three-Phase Power Electronic Systems

Research Article

Mateusz Dybkowski, Kamila Anna Jankowska

Department of Electrical Machines, Drives and Measurements, Wroclaw University of Science and Technology, 50-370 Wroclaw, Poland

Received: October 21, 2022; Accepted: November 15, 2022

Abstract: The article discusses the universal current sensor fault detection and compensation mechanism, which can be applied in three-phase power electronics (PE) symmetrical system. The mechanism is based on the assumption that a symmetrical system can be described using different components in the stationary reference frame. The solution given in article as a Cri-base detector was tested in electrical drives with induction motors (IMs) and permanent magnet synchronous motors (PMSMs). This study also proves that the same algorithm can work stable in active rectifier systems. Such an application of this detector has not been previously reported in the literature. The article describes the detection of various types of faults in different phases. The fault-tolerant voltage-oriented control (FTVOC) of an active rectifier is compared with previously described solutions for IMs and PMSMs. By analysing in various types of systems, the work proves the universality of the detector based on Cri markers.

Keywords: *FTC • active rectifier • current sensor • PMSM • IM • Diagnostic*

1. Introduction

Fault-tolerant electrical energy conversion systems are being examined in many research studies around the world (Kaźmierowski and Tunia, 1994). All systems, AC–DC, AC–DC–AC and DC–DC, were analysed and tested from different points of view (Berriri et al., 2012; Betta and Pietrosanto, 2000; Blanke et al., 2003; Choi and Lee, 2020; Gaeid and Ping, 2011; Isermann, 2006; Jiang and Xiang, 2012; Kowalski et al., 2013; Tallam et al., 2007; Tsai et al., 2020).

Many publications describe the fault-tolerant control systems (FTCS), for both power electronics (PE) (Abdelrahem et al., 2020; Jung et al., 2019) and measurement systems, which are necessary for the proper operation of FTCS. Thus, the issue of incipient fault detection and compensation has recently become one of the basic requirements for modern PE systems (Jiang, 2011; Lee and Ryu, 2003). Measurement sensors are necessary for the proper operation of modern power electronic systems and drive systems (Fuchs, 2003; Shicai and Jianxiao, 2012), both of which are measuring systems of AC and DC signals as well as signals such as mechanical vibrations and angular velocity. The measuring equipment is not a reliable system. In the PE system, current and voltage sensors are necessary for the proper working of vector control algorithms (Adamczyk and Orlowska-Kowalska, 2019; Bahri et al., 2007; Knapczyk and Pienkowski, 2010; Patan et al., 2020).These sensors are very sensitive and may break (Blanke et al., 2003; Shicai and Jianxiao, 2012; Tsai et al., 2020).

Industrial system breakdowns occur frequently, which can even cause damage to the control system and PE in extreme cases (Jung et al., 2019). Therefore, it is important to develop techniques for the detection of damage in measuring elements and for their compensation. There are more and more works related to systems with an increased degree of security, that is, the so-called fault-tolerant system.

* *Email: kamila.jankowska@pwr.edu.pl*

The article focuses on the analysis of the operation of a universal detection system that can be used in vector-controlled induction motor (IM) drives, permanent magnet synchronous motor (PMSM) drives and active rectifiers controlled by voltage-oriented control (VOC). A fault detection algorithm of the current sensors based on Cri markers was proposed, but so far, it has been analysed only in drive systems with IMs (Dybkowski and Klimkowski, 2016) and PMSMs (Jankowska and Dybkowski, 2021, 2022). It has been shown that the detector is highly universal and can be used in any three-phase system, assuming that it is symmetrical. The simulation and experimental studies are presented. The simulation was performed using MATLAB Simulink (IM and PMSM analysis) and PSIM (active rectifier analysis). The experimental tests were carried out on a stand with the DS1103 and DS1202 cards from dSpace.

2. Universal Current Detection and Compensation System

In the analysed systems, with IM, PMSM and active rectifier, three current sensors—one for each phase—are used. For the control in the 'healthy' condition, only two sensors are used. Grid current sensor (in electrical drives the stator current sensor) faults can be detected based on the following equation:

$$\left|i_A + i_B + i_C\right| = f_0 \tag{1}$$

$$IF \quad f_0 < \varepsilon_0 \quad THEN \quad f_i = 0 \quad ELSE \quad f_i = 1 \tag{2}$$

where ε_0 is a small constant.

For the faulty grid sensor, the coefficient f_i = 1. This explains the grid current sensor faults or other abnormalities in the measuring system. Based on this information, it cannot be clearly identified which sensor is broken. It is necessary to add additional information to the fault detection algorithm. Locating the faulty sensor is necessary in order to compensate for the failure.

This section of the article analyses the method proposed in Dybkowski and Klimkowski (2016) and tested in Jankowska and Dybkowski (2021, 2022), which is a modification of the detection system proposed in Bahri et al. (2007), which guarantees the detection of a broken sensor.

This algorithm is based on the fact that grid (or stator) current transformation from the ABC frame to the stationary reference frame (α-β) can be obtained using different equations.

For the symmetrical three-phase system, the grid currents in the α-β frame can be calculated from the following equations based on two or three grid sensors:

$$i_{s\alpha 1} = \frac{2}{3}\left(i_{sA} - \frac{1}{2}(i_{sB} + i_{sC})\right),\ i_{s\beta 1} = \frac{\sqrt{3}}{3}(i_{sB} - i_{sC}) \tag{3}$$

$$i_{s\alpha 2} = i_{sA},\ i_{s\beta 2} = \frac{\sqrt{3}}{3}\left(i_{sA} + 2i_{sB}\right) \tag{4}$$

$$i_{s\alpha 3} = -\left(i_{sB} + i_{sC}\right),\ i_{s\beta 3} = -\frac{\sqrt{3}}{3}\left(i_{sA} + 2i_{sC}\right) \tag{5}$$

It can be seen that each of the previous equations determining the current components depends on the specific currents in A, B, and C phases. It can also be seen that some components are independent of the sensor in the A or B or C phase. The analysis is presented in Table 1.

Based on Eqs (3)–(5), it is possible to identify the three markers $C_{ri1\text{-}3}$ Eq. (6):

$$C_{ri1} = \left(i_{s\alpha 3}^2 + i_{s\beta 1}^2\right),\ C_{ri2} = \left(i_{s\alpha 2}^2 + i_{s\beta 3}^2\right),\ C_{ri3} = \left(i_{s\alpha 2}^2 + i_{s\beta 2}^2\right) \tag{6}$$

These signals can define the sensitivity to the failure of the current sensor in one phase.

It can be observed that those equations depend only on two grid currents:

$$C_{ri1} = \left(-\left(i_{sB} + i_{sC}\right)\right)^2 + \left(\frac{\sqrt{3}}{3}\left(i_{sB} - i_{sC}\right)\right)^2 \Rightarrow \quad C_{ri1} = f\left(i_{sB}, i_{sC}\right) \tag{7}$$

$$C_{ri2} = \left(i_{sA}\right)^2 + \left(-\frac{\sqrt{3}}{3}\left(i_{sA} + 2i_{sC}\right)\right)^2 \Rightarrow \quad C_{ri2} = f\left(i_{sA}, i_{sC}\right) \tag{8}$$

$$C_{ri3} = \left(i_{sA}\right)^2 + \left(\frac{\sqrt{3}}{3}\left(i_{sA} + 2i_{sB}\right)\right)^2 \Rightarrow \quad C_{ri3} = f\left(i_{sA}, i_{sB}\right) \tag{9}$$

During “normal’ operations, when the current sensors are ‘healthy’, the relation between stator current components can be obtained by the following relation:

$$\left(i_{s\alpha 1} = i_{s\alpha 2} = i_{s\alpha 3}\right) \wedge \left(i_{s\beta 1} = i_{s\beta 2} = i_{s\beta 3}\right) \tag{10}$$

Table 2 shows the dependence of the marked markers on the sensors in individual phases.

It can be observed that each marker Cri is sensitive to the two sensor faults. It means that if the sensor in one phase is damaged, it is not only possible to identify this fact but also to indicate which sensor is broken Knapczyk and Pienkowski, 2010.

The proposed solution can be applied in the open- and closed-loop systems, but in this case, detection must be done in the first two samples, which was proved by previous studies (Dybkowski and Klimkowski, 2016; Jankowska and Dybkowski, 2021, 2022).

In realisation, if this detector is used in the microprocessor systems, the difference between chosen markers must be analysed Eq. (11).

$$\Delta C_{rij} = \left| C_{rij}(k) - \Delta C_{rij}(k-1) \right| \quad for \quad j = 1,2,3 \tag{11}$$

This allows determining which marker is not sensitive to the sensor failure. In Tables 3 and 4, the relationships between the various deviations of ΔC_{ri1}, ΔC_{ri2} and ΔC_{ri3} are presented.

Table 1. Influence of the current sensor faults on the sensitivity of α-β currents.

Components α-β	i_{sA}	i_{sB}	i_{sC}
$i_{s\alpha 1}$	Sensitive	Sensitive	Sensitive
$i_{s\alpha 2}$	Sensitive	Insensitive	Insensitive
$i_{s\alpha 3}$	Insensitive	Sensitive	Sensitive
$i_{s\beta 1}$	Insensitive	Sensitive	Sensitive
$i_{s\beta 2}$	Sensitive	Sensitive	Insensitive
$i_{s\beta 3}$	Sensitive	Insensitive	Sensitive

Table 2. Influence of current sensor faults on the sensitivity of C_{ri} markers.

Markers	i_{sA}	i_{sB}	i_{sC}
C_{ri1}	Insensitive	Sensitive	Sensitive
C_{ri2}	Sensitive	Insensitive	Sensitive
C_{ri3}	Sensitive	Sensitive	Insensitive

Table 3. Relationships between the various deviations of ΔC_{ri1}, ΔC_{ri2} and ΔC_{ri3} for IM and active rectifier.

Broken sensor	C_{rik}	D_1	D_2	D_3	Stator currents
None	$\Delta C_{ri1} = \Delta C_{ri2} = \Delta C_{ri3}$	0	0	0	*Any*
i_A	$\Delta C_{ri1} < \Delta C_{ri2} < \Delta C_{ri3}$	1	0	0	$i_{s\alpha3}$, $i_{s\beta1}$
i_B	$\Delta C_{ri2} < \Delta C_{ri3} < \Delta C_{ri1}$	0	1	0	$i_{s\alpha2}$, $i_{s\beta3}$
i_C	$\Delta C_{ri3} < \Delta C_{ri2} < \Delta C_{ri1}$	0	0	1	$i_{s\alpha2}$, $i_{s\beta2}$

IM, induction motor.

Table 4. Relationships between various deviations of ΔC_{ri1} and ΔC_{ri2} for PMSM.

Broken sensor	C_{rik}	D_1	D_2	Stator currents
None	$\Delta C_{ri1} = \Delta C_{ri2} = \Delta C_{ri3}$	0	0	*Any*
i_A	$\Delta C_{ri1} < \Delta C_{ri3} < \Delta C_{ri2}$	1	0	$i_{s\alpha3}$, $i_{s\beta1}$
i_B	$\Delta C_{ri2} < \Delta C_{ri3} < \Delta C_{ri1}$	0	1	$i_{s\alpha2}$, $i_{s\beta3}$

PMSM, permanent magnet synchronous motor.

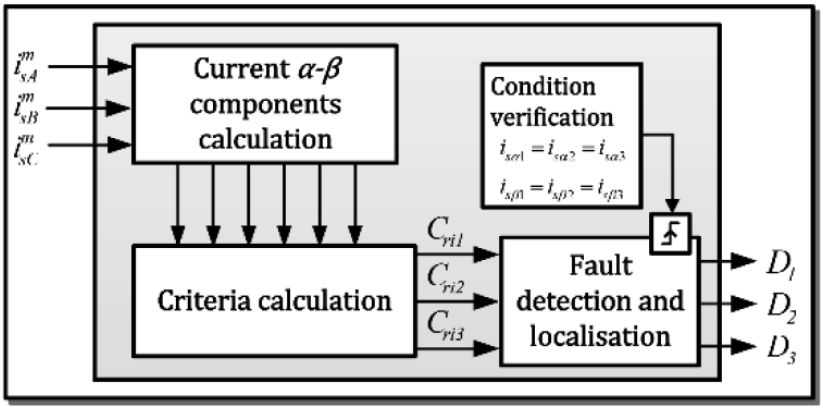

Fig. 1. Current sensor fault detector scheme.

If signals $\Delta C_{ri1} = \Delta C_{ri2} = \Delta C_{ri3}$, all current sensors are healthy, and for this case, any current sensor can be used for transformation.

If those signals are not equal according to Tables 3 and 4, only two healthy sensors can be used in the control system for current transformation. Furthermore, it is possible to detect which sensor is broken. In the case of the active rectifier and IM, damage was examined in three phases, while for the PMSM, damage was examined in two phases (A and B). The relationships between the markers indicate that damage in the conducted tests differs because they were performed in different laboratory set-ups.

The general detection scheme is the same for all tested systems and is presented in Figure 1.

3. Detection and Compensations of the Current Sensor Fault in the Vector Control Algorithm

As already mentioned, the marker-based detection system was tested in electrical drive systems with IMs and PMSMs. The analyses were carried out for the drives shown in Figure 2. The issue of the possibility of application of this solution in active rectifier systems has not been presented before and is the closure of the topic, showing the universality of the described solution. From this point of view, it is an original topic.

The direct field-oriented control (DFOC) structure with the space vector modulation algorithm (DFOC) (Adamczyk and Orlowska-Kowalska, 2019; Kowalski et al., 2013) is presented in Figure 2a. In this structure, which is used in the simulation and experimental tests, the classical PI controllers are used. The incremental encoder is applied to the rotor speed measure (resolution is equal to 5,000 imp/rpm). Stator voltage is calculated from DC bus voltage. A similar structure, used in simulation and experimental tests of the proposed detection system, for PMSMs is presented in Figure 2b.

The VOC structure with a space vector modulation algorithm (VOC) (Choi and Lee, 2020; Tsai et al., 2020), with the current sensor fault detection system, is presented in Figure 3.

To measure stator or grid currents, the closed-loop hall effect current sensors are used. The scheme of this type of a sensor is demonstrated in Figure 4.

In the analysed systems, three current sensors can be used for the calculation of the current components in a stationary reference frame.

It is obvious that in each vector control algorithm in the three-phase symmetrical systems, only two sensors are necessary for current transformation. For safety reasons, an additional redundant sensor can be used.

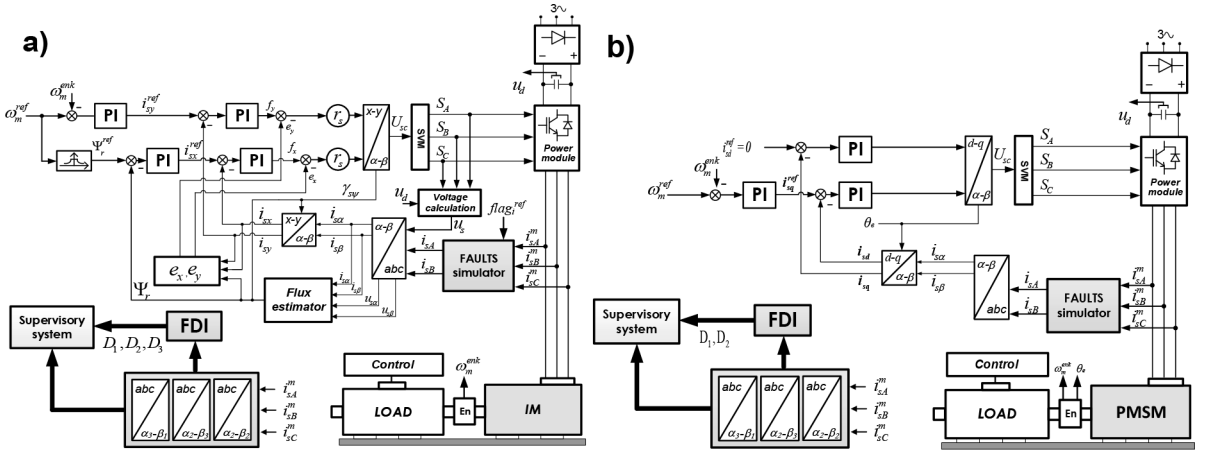

Fig. 2. Scheme of the DFOC structure for IM (a) and PMSM (b). DFOC, direct field-oriented control; IM, induction motor; PMSM, permanent magnet synchronous motor.

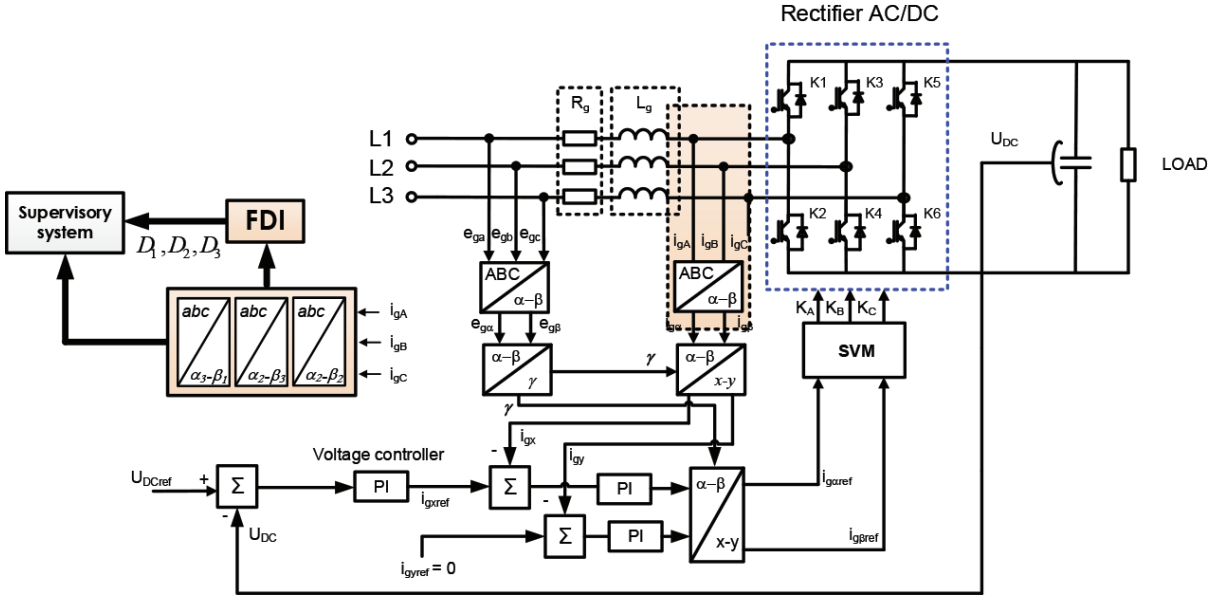

Fig. 3. Scheme of a VOC structure. VOC, voltage-oriented control.

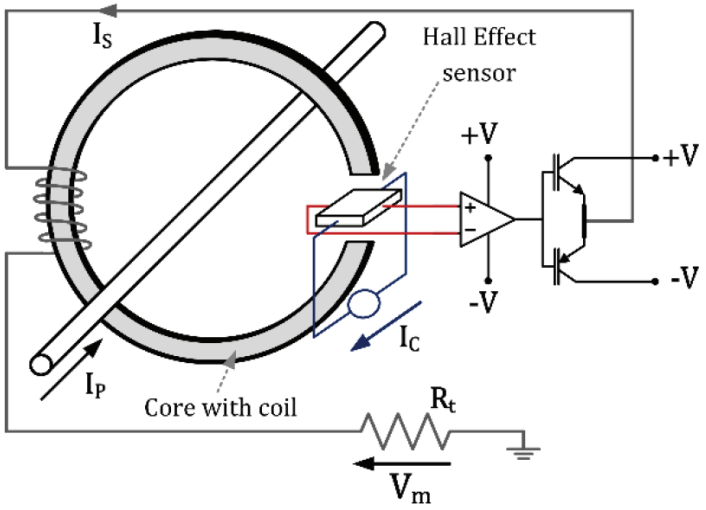

Fig. 4. Closed-loop hall effect current sensor scheme (Patel and Ferdowsi, 2009).

In the field-oriented control (FOC) and VOC, the information about grid (stator) currents is necessary for the proper operation. Each incorrect information from the closed-loop hall effect current sensor can be visible in the output controlled signal. In this study, it was assumed that each current sensor can

- be totally broken,
- generate noise, and
- contain gain error (20% of the nominal signal [offset]).

A mathematical interpretation of these types of faults can be obtained by the following equation (example for phase B):

$$i_B = I_m \sin(\omega t + \varphi) \tag{12}$$

where I_m is the current amplitude, $\omega = 2\pi f$, f is the frequency, and ϕ is the initial phase.

In Figure 5a, markers $C_{ri1\text{-}3}$ for a totally broken current sensor in phase B (VOC system) are presented. It is visible that during faulty conditions, the effect is visible in the first two samples.

Markers $C_{ri1\text{-}3}$ can be used also for the detection of other kinds of sensor faults. In Figures 5b and 5c, markers $C_{ri1\text{-}3}$ for gain offset and noise in phase B are presented (similar results can be obtained for each phase). It was demonstrated in previous studies (Dybkowski and Klimkowski, 2016; Jankowska and Dybkowski, 2021, 2022) and is shown in experimental results in Figures 6 and 7.

In the next section of the article, the fault-tolerant voltage-oriented control (FTVOC) algorithm is analysed during a current sensor fault. Simulation results are presented. In the sensor fault detection, the algorithm presented in this article is used. During the normal operation, only two sensors are used in the closed-loop system (current in phases A and B). After fault detection, the faulty sensor is replaced by the grid current sensor from phase C. Based on the information from the detection algorithm, the proper transformation is used.

The normal operation of the vector-controlled active rectifier is presented in Figure 8. It is visible that the system is set to 200 V. For t = 0.15 s, the additional load is switched. Component i_{gy} of the grid current is kept at zero. During this test, currents A and B were used to calculate the current in the stationary reference frame.

Figure 9 presents the results of the VOC rectifier system with a totally broken current sensor in phase A. In this test, the two current sensors were used in the control system. Current components $i_{s\alpha}$ and $i_{s\beta}$ were calculated from the information from sensors in phases A and B.

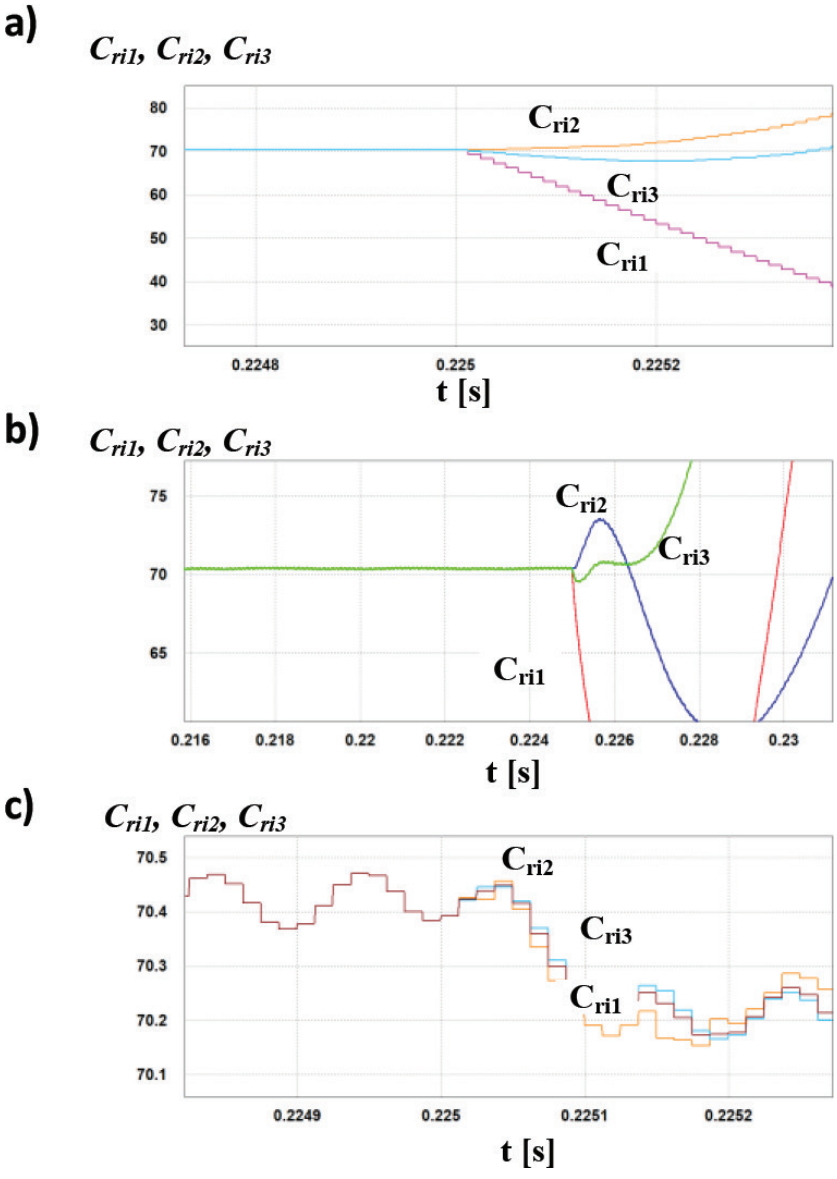

Fig. 5. Transients of markers $C_{ri1\text{-}3}$ during the current sensor fault [totally broken sensor (a), gain error (b), and offset (c)] for phase B.

In the analysed situation, the current sensor was broken at t = 0.225 s. After faults, the symptoms are visible on the current transients. It is visible that the system is not stable during this fault. Voltage in the DC bus is not kept in the reference value. Other signals are not controlled either. From the safety point of view, this kind of the fault is the most dangerous for the systems receiving feedback from the measured currents. Similar results can be obtained for the totally broken sensor in the phase B.

Another kind of a faulty operation was demonstrated in Figures 10 and 11. The analysis is presented with the noise and offset. Such kinds of faults are not so dangerous as a totally broken sensor; however, oscillation of the controlled signals can be visible. Even these kinds of faults can eliminate a rectifier from an industrial system. The faults must be detected and compensated the same as the most dangerous total lack of the signal from current sensors.

Costs are of secondary importance in fault-tolerant systems. Therefore, in these systems, it is necessary to provide either hardware or analytical redundancy. This article presents the stator current sensor fault detection system that was previously presented for drives with IMs and showed very good properties (Dybkowski and Klimkowski, 2016).

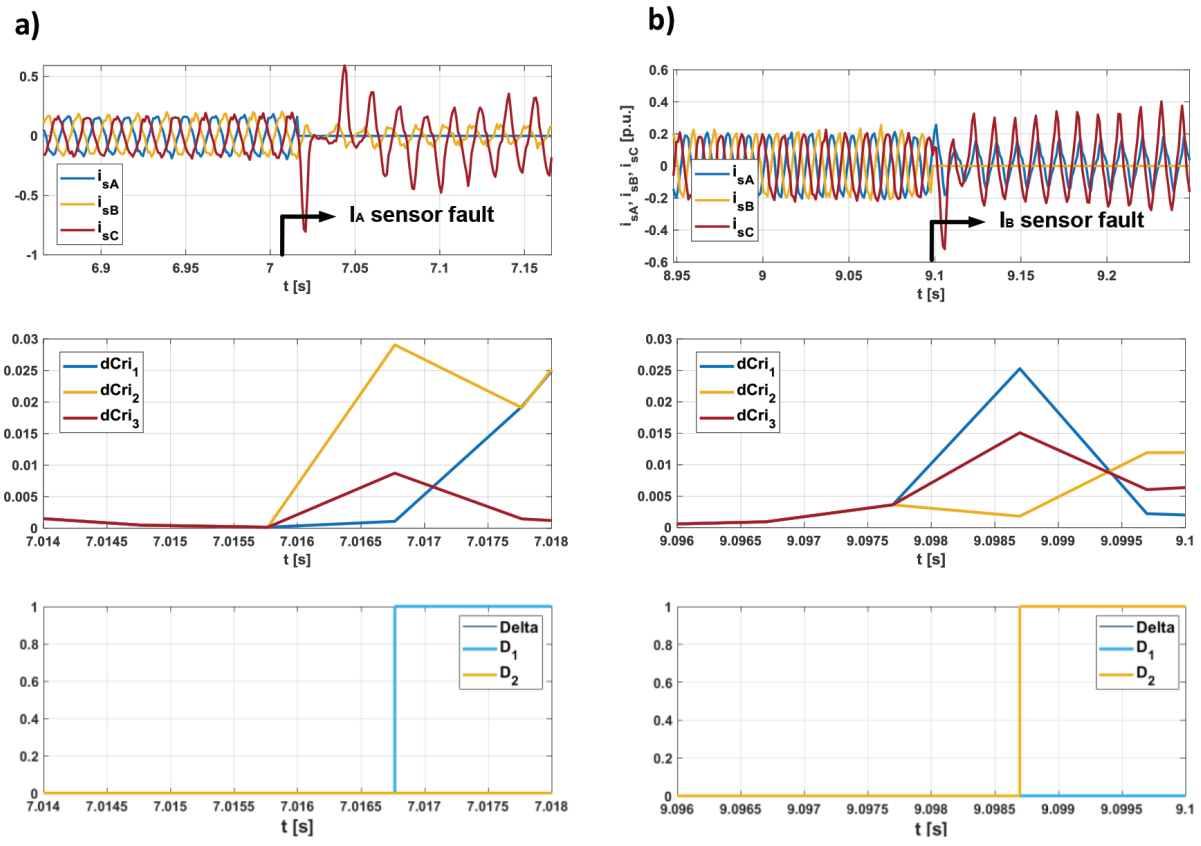

Fig. 6. Marker transients in PMSM drive under lack of signal in phase A (a) and phase B (b) (results for FOC). FOC, field-oriented control; PMSM, permanent magnet synchronous motor.

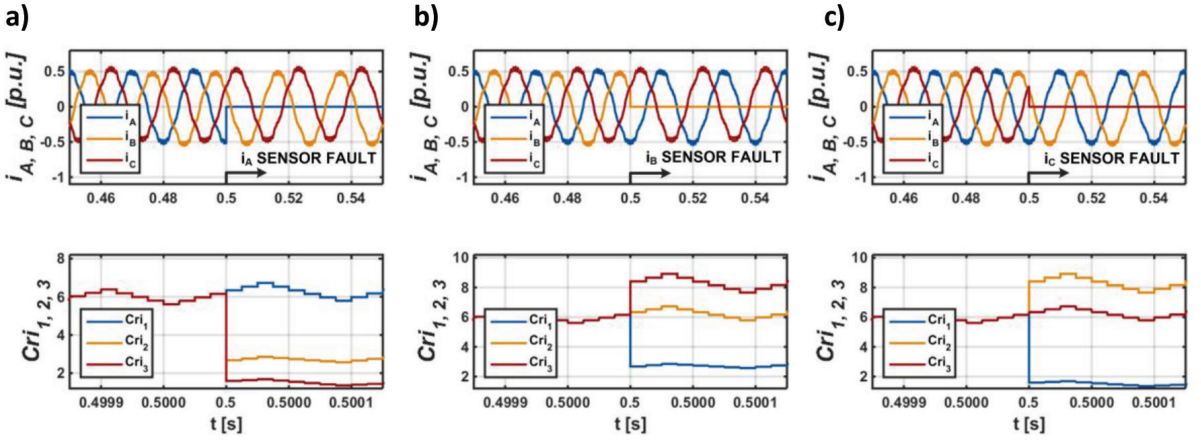

Fig. 7. Transients of the stator current in phases A, B and C and markers $C_{ri1\text{-}3}$ during current sensor fault in DFOC of IMs (totally broken sensor) for phases A (a), B (b) and C (c) (results for scalar control) (Dybkowski and Klimkowski, 2016). DFOC, direct field-oriented control; IMs, induction motors.

As shown in the analysis presented in Figures 11 and 12, the detection algorithm can detect faults during the first two steps after faulty conditions. This means that after this time, the proposed algorithm can detect a false signal. In the closed-loop VOC, the system can compensate some signals behaviours and the symptoms are not obvious.

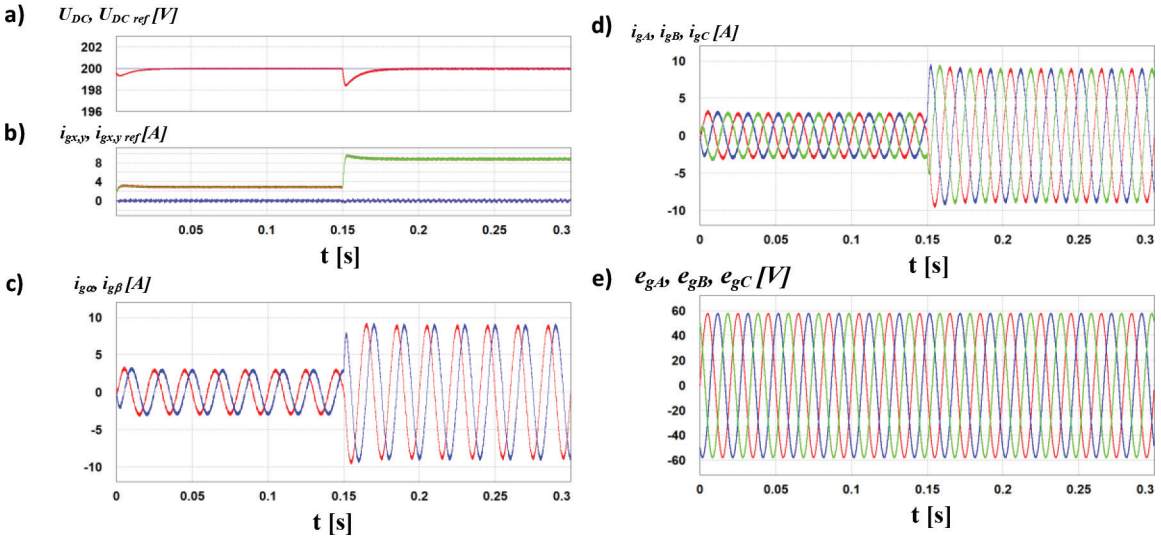

Fig. 8. Results for VOC of an active rectifier under normal operations (sensor in phases A and B are 'healthy'), DC bus voltage (a), currents x, y (b), currents, (c), ABC currents (d) and ABC voltages (e). VOC, voltage oriented control.

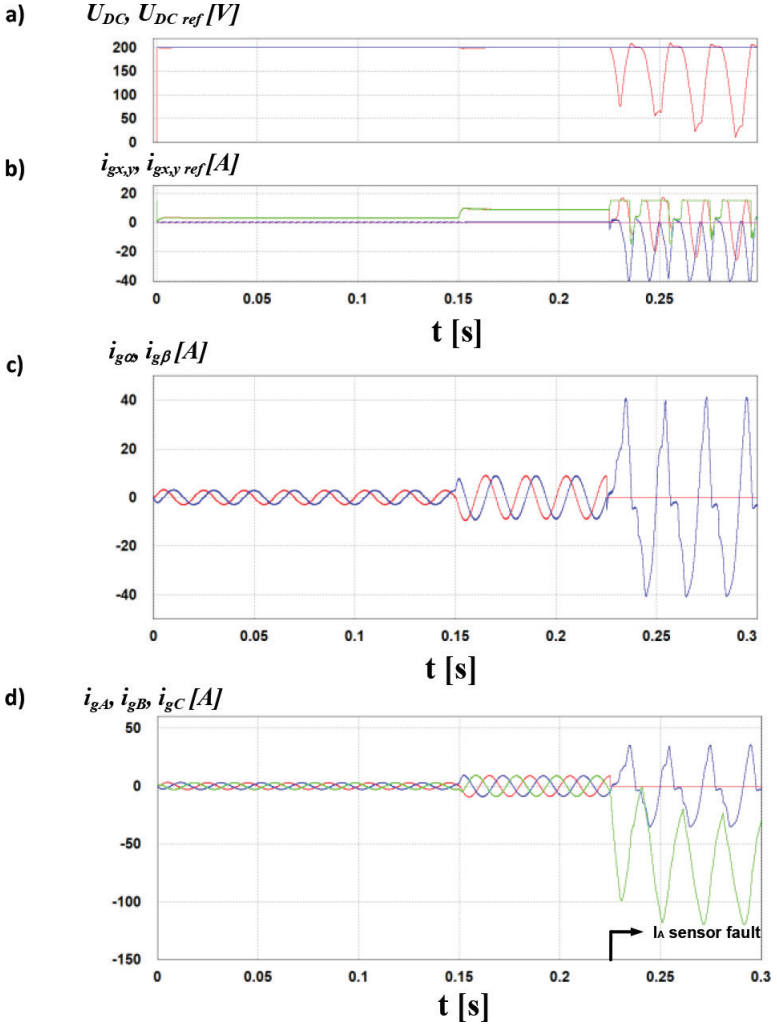

Fig. 9. Results for VOC of an active rectifier with a totally broken current sensor in phase A, iA' = 0, DC bus voltage (a), currents x, y (b), currents α,β, (c) and ABC currents (d). VOC, voltage-oriented control.

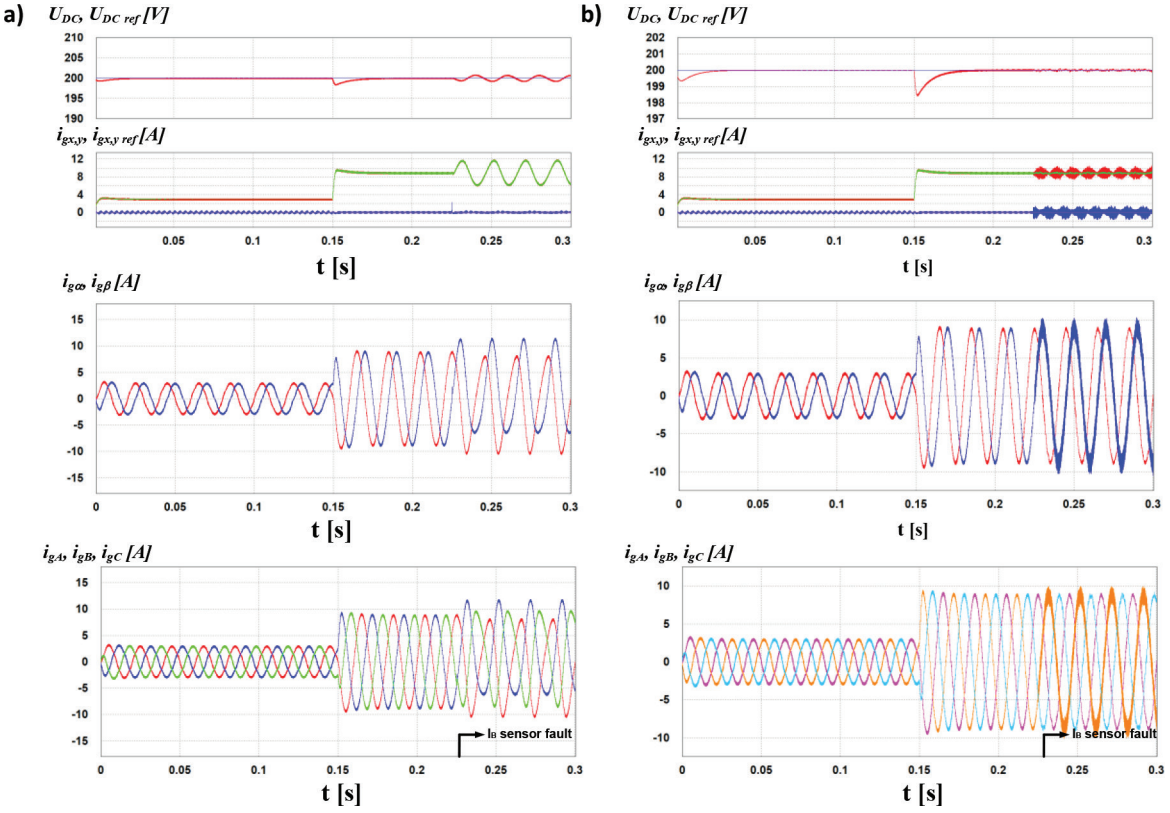

Fig. 10. Results for the VOC of the active rectifier with gain error in the current sensor in phase B, $i_B' = (1 \pm N) I_m \sin(\omega t + \varphi)$ (a) and noise in the current sensor in phase B, $i_B' = I_m \sin(\omega t + \varphi) + n(t)$ (b). VOC, voltage oriented control.

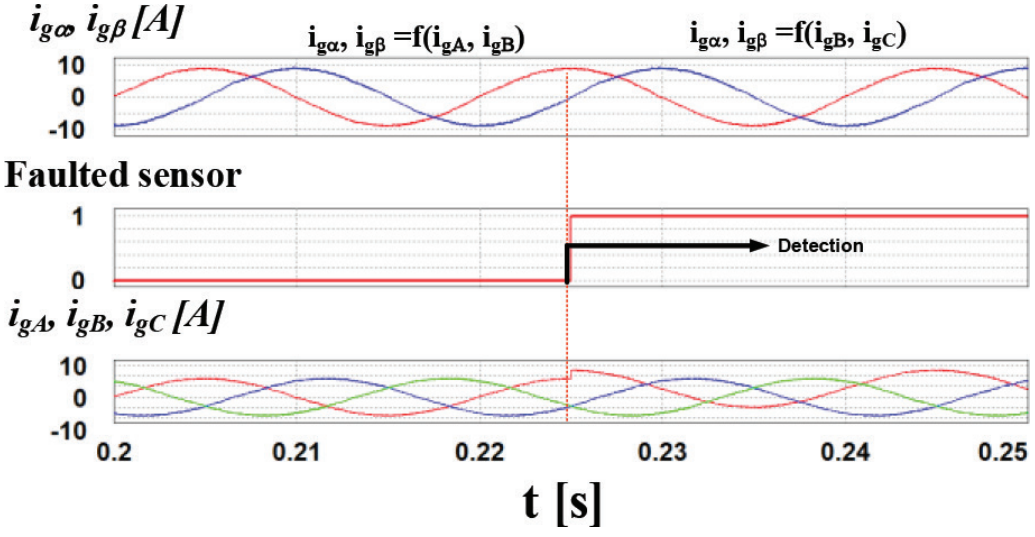

Fig. 11. Transients of state variables of VOC during current sensor fault (offset 2 A) for phase A. VOC, voltage oriented control.

The most important advantage of the proposed algorithm is the fact that the detection is taken in the first samples after the fault. It can be observed in Figures 11 and 12 that in the current transients and current components, no effect of the faulty conditions is visible. The detection time is equal to two steps of the calculation time. The same effect presented in Dybkowski and Klimkowski (2016).

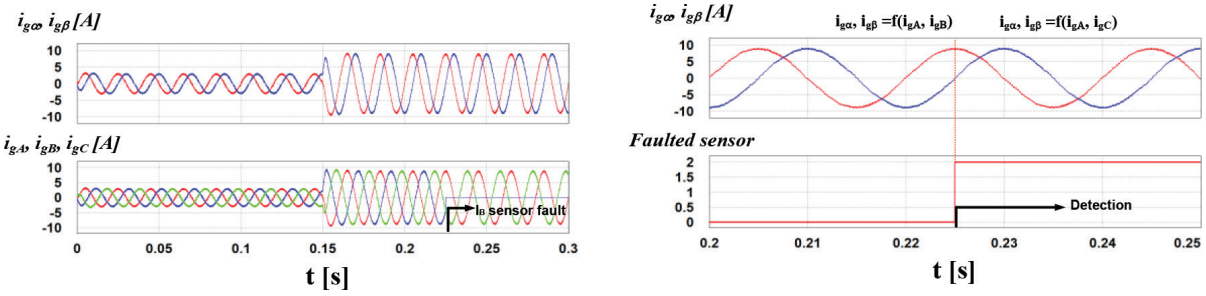

Fig. 12. Transients of state variables of VOC during current sensor faults (totally broken sensor) for phase B. VOC, voltage oriented control.

Each kind of sensor fault is detected and compensated. In all cases, the sensor fault was detected, and the system was reconfigured—another current sensor was used for the stationary current calculation.

4. Conclusion

In this article, the FTC system for VOC was presented. The detection algorithm for the current grid sensor faults was presented and described in detail. The detection algorithm is based on a simple mathematical relationship between currents in grid phases A, B and C, and stator current components in a stationary reference frame. The proposed methodology is universal and can be applied in the drive system with an IM and also for the rectifier systems controlled by the vector methods. The analysis presented in this article shows that it is possible to detect and compensate for the grid current during very a short time period. The effect of the fault is not visible in the state variables. The proposed system can operate as a stand-alone detection system or as a compensation algorithm in a full FTC system.

References

Abdelrahem, M., Rodríguez, J. and Kennel R. (2020). Improved Direct Model Predictive Control for Grid-Connected Power Converters. *Energies*, 13, p. 2597.

Adamczyk, M. and Orlowska-Kowalska, T. (2019). Virtual Current Sensor in the Fault-Tolerant Field-Oriented Control Structure of an Induction Motor Drive. *Sensors*, 19, p. 4979.

Bahri, I., Naouar, M., Slama-Belkhodja, I. and Monmasson, E. (9-12.09.2007). FPGA-based FDI of faulty current sensor in current controlled PWM converters. In: *The International Conference on "Computer as a Tool*". Warszawa: EUROCON.

Berriri, H., Naouar, M. W. and Slama-Belkhodja, I. (2012). Easy and Fast Sensor Fault Detection and Isolation Algorithm for Electrical Drives. *IEEE Trans. on Power Electronics*, 27(2), pp. 490–499.

Betta, G. and Pietrosanto, A. (2000). Instrument Fault Detection and Isolation: State of the Art and New Research Trends. *IEEE Transactions on Instrumentation and Measurement*. 49(1), pp. 100–107.

Blanke, M., Kinnaert, M. and Lunze, J. (2003). *Diagnosis and Fault-Tolerant Control*: Springer-Verlag.

Choi, J. and Lee, S. J. (2020). A Sensor Fault-Tolerant Accident Diagnosis System. *Sensors*, 20, p. 5839.

Dybkowski, M. and Klimkowski, K. (25-30.09.2016). Stator current sensor fault detection and isolation for vector controlled induction motor drive. In: *2016 IEEE International Power Electronics and Motion Control Conference (PEMC)*. Varna, Bulgaria: IEEE, pp. 1097—1102.

Fuchs, F. W. (2003). Some diagnosis methods for voltage source inverters in variable speed drives with induction machines-a survey. IECON'03. *29th Annual Conference of the IEEE Industrial Electronics Society* (IEEE Cat. No. 03CH37468). Vol. 2. IEEE.

Gaeid, K. S. and Ping, H. W. (2011). Fault Tolerant Control of Induction Motor. *Modern Applied Science*, 5(4), pp. 83–94.

Isermann, R. (2006). *Fault Diagnosis Systems. An Introduction from Fault Detection to Fault Tolerance*. New York: Springer.

Jankowska, K. and Dybkowski, M. (2021). A Current Sensor Fault Tolerant Control Strategy for PMSM Drive Systems Based on Cri Markers. *Energies*, 14(12), art. 3443, pp. 1–18.

Jankowska, K. and Dybkowski, K. (2022). Experimental Analysis of the Current Sensor Fault Detection Mechanism Based on Cri Markers in the PMSM Drive System. *Applied Sciences*, 12(9), art. 9405, pp. 1–18.

Jiang, L. (2011). *Sensor Fault Detection and Isolation using System Dynamics Identification Techniques*. PhD thesis. The University of Michigan.

Jiang, J. and Xiang, Y. (2012). Fault-Tolerant Control Systems: A Comparative Study Between Active and Passive Approaches. *Annual Reviews in Control,* 36(1), pp. 60–72.

Jung, J.-H., Ku, H.-K., Son, Y.-D. and Kim, J.-M. (2019). Open-Switch Fault Diagnosis Algorithm and Tolerant Control Method of the Three-Phase Three-Level NPC Active Rectifier. *Energies*, 12, p. 2495.

Kaźmierowski, M. P. and Tunia, H. (1994). *Automatic Control of Converter-Fed Driver*. Warsaw, Amsterdam, New York, Tokyo: PWN-Elsevier Science Publishers.

Knapczyk, M. and Pienkowski, K. (2010). Sliding-Mode Virtual Flux-Oriented Control of PWM Rectifier with DC-Bus Voltage and Current Sensors. *Variations*, 4(6), p. 7.

Kowalski, C. T., Wierzbicki, R., Wolkiewicz M. (2013). Stator and Rotor Faults Monitoring of the Inverter-Fed Induction Motor Drive using State Estimators, Automatika, Vol 54, No 3.

Lee, K. S. and Ryu, J. S. (2003). Instrument Fault Detection and Compensation Scheme for Direct Torque Controlled Induction Motor Drivers. *IEE Proceedings-Control Theory and Applications*, 150(4), pp. 376–382.

Patan, K., Patan, M. and Klimkowicz, K. (2020). Sensor Fault-Tolerant Control Design for Magnetic Brake System. *Sensors*, 20, p. 4598.

Patel, A. and Ferdowsi, M. (2009). Current Sensing for Auto-motive Electronics—A Survey. *IEEE Transactions on Vehicular Technology*, 58(8), pp. 4108–4119.

Shicai, F. and Jianxiao, Z. (2-5.06.2012). Sensor fault detection and fault tolerant control of induction motor drivers for electric vehicles. In: *IEEE 7th Int. Power Electronics and Motion Control Conference—ECCE Asia*. China, pp. 1306–1309.

Tallam, R. M., Lee, S. B., Stone, G. C., Kliman, G. B., Yoo, J. Y., Habetler, T. G. and Harley, R. G. (2007). A Survey of Methods for Detection of Stator Related Faults in Induction Machines. *IEEE Transactions on Industry Applications*, 43(4), pp. 920–933.

Tsai, M.-F., Tseng, C.-S. and Lin, B.-Y. (2020). Phase Voltage-Oriented Control of a PMSG Wind Generator for Unity Power Factor Correction. *Energies*, 13, p. 5693.